Elimination of Spurious Loss in Euler Equation Computations

Mark Drela * Ali Merchant † Jaime Peraire *
MIT Department of Aeronautics and Astronautics

Abstract

The accuracy of a standard implicit conservative Euler equation solver is greatly improved by incorporation of an entropy-conservation equation, used in lieu of the streamwise momentum equation in all regions of the flow except at shock waves. A slight modification is also required at stagnation points to maintain well-posedness. The overall method completely eliminates spurious entropy errors, and thus reduces the grid density required to achieve any particular level of accuracy. Results are presented for subsonic and transonic airfoil flows.

Although the derivation and results are for 2-D Euler equations, the approach has no inherent limitations which preclude extension to 3-D or viscous flows. A brief discussion of these extensions is presented.

Nomenclature

c	speed of sound
E	total energy
H	total enthalpy
h	static enthalpy
ℓ	cell size
M	Mach number
p	pressure
$\vec{Q}$	enthalpy flux
q	speed $(= \lvert\vec{q}\rvert)$
$\vec{q}$	velocity vector
S	entropy
u, v	velocity components
α	angle of attack
γ	specific-heat ratio
$\vec{\delta}(\,)$	upwinding change
ε	viscous dissipation
λ	characteristic speed
ρ	mass density
$\bar{\bar{\tau}}$	shear stress tensor

* Associate Professor, AIAA Associate Fellow.
† Research Assistant.

1 Introduction

Most current Euler equation solution methods solve the mass, momentum, and energy equations discretized in strongly-conservative form.

$$\frac{\partial \rho}{\partial t} + \nabla \cdot (\rho \vec{q}) = 0 \tag{1}$$

$$\frac{\partial (\rho u)}{\partial t} + \nabla \cdot (\rho \vec{q} u + p\hat{\imath}) = 0 \tag{2}$$

$$\frac{\partial (\rho v)}{\partial t} + \nabla \cdot (\rho \vec{q} v + p\hat{\jmath}) = 0 \tag{3}$$

$$\frac{\partial (\rho E)}{\partial t} + \nabla \cdot (\rho \vec{q} H) = 0 \tag{4}$$

The velocity vector $\vec{q}$ and its magnitude q are defined in terms of the cartesian velocity components,

$$\vec{q} = u\hat{\imath} + v\hat{\jmath}$$
$$q^2 = u^2 + v^2$$

where the flow variables are defined as usual.

$$p = (\gamma - 1)\left(\rho E - \frac{1}{2}\rho q^2\right)$$
$$H = E + \frac{p}{\rho} = h + \frac{1}{2}q^2$$
$$c^2 = \frac{\gamma p}{\rho}$$
$$M = \frac{q}{c}$$

The mass, momentum, and energy equations above can be combined to yield the entropy conservation equation

$$\frac{\partial (\rho S)}{\partial t} + \nabla \cdot (\rho \vec{q} S) = 0 \tag{5}$$

$$\text{where} \qquad S \equiv \ln\left(\frac{h^{\gamma/(\gamma-1)}}{p}\right) \tag{6}$$

which shows that the entropy S should be constant throughout the flow if it is constant at the upstream boundary. In practice, however, the discrete forms of equations (1,2,3,4) must be stabilized with dissipative terms, which either appear naturally as truncation errors or are added explicitly, depending on the discretization scheme used. With the additional dissipative terms, equation (5) will now have a positive source term on the righthand side, giving entropy generation along streamlines. This loss production is "correct" only at shocks, where the dissipative terms correctly model real viscous processes. Away from shocks, however, the additional terms produce spurious losses which degrade solution accuracy.

The entropy-conservation equation (5) is used to replace the streamwise momentum equation in the viscous/inviscid MSES Euler code [1], in all regions of the flow except at shocks. Spurious losses are thus eliminated, allowing acceptable solutions on extremely coarse grids. Other loss-mitigation techniques have been presented by Lee and Chu [2] who employ a Clebsch velocity decomposition, and by Denton and Xu [3] who employ the entropy conservation equation with an ad-hoc source term at shocks. More recently, Hafez and Guo [4] have presented an formulation using a relaxation scheme of the Cauchy/Riemann equations for the velocity components, which have the total enthalpy and the entropy in their source terms. The entropy is updated by solving an entropy convection equation downstream of shocks. The total enthalpy is assumed constant, although its convection equation could easily be employed instead.

All these previous approaches have assumed a particular topology of the flow, or have been restricted to special types of solution schemes. The MSES code [1] is strictly for steady 2-D flows, using a streamline grid and a very restricted form of dissipation not suitable for more general fixed-grid solvers or for 3-D. The scheme of Lee and Chu [2] uses streamline tracing to solve the convection equations, loosely coupled to an iterative scheme for the Clebsch velocity potential. Denton and Xu [3] report poor stability near $M = 0$, and do not show any solutions with well-resolved stagnation points. It is not clear that their scheme is consistent. The method of Hafez and Guo [4] requires knowledge of the location and orientation of shocks to produce the appropriate entropy sources for the entropy convection equation. This can lead to difficulties at intersecting shocks, especially in 3-D. The singular nature of the Cauchy/Riemann equations at stagnation points is not addressed.

The remainder of this paper will focus on the formulation of an entropy-conserving method for general 2-D or 3-D Euler solvers using unstructured grids. The assumptions of steady flow or constant total enthalpy will not be required. Only the approximate location of shocks will be required — knowledge of shock orientation will not be necessary. The issue of consistency, and well-posedness at stagnation points will be addressed in considerable detail. Results for subsonic and transonic 2-D Euler flows will be presented. Extensions to 3-D and Navier-Stokes solvers will also be discussed.

2 Discrete Formulation and Artificial Dissipation

A fairly general way to describe upwinded conservative schemes is to include a dissipative upwinding change to each flux component.

$$\frac{\partial \rho}{\partial t} + \nabla \cdot \left[\rho \vec{q} - \lambda \vec{\delta} \rho \right] = 0 \tag{7}$$

$$\frac{\partial (\rho u)}{\partial t} + \nabla \cdot \left[\rho \vec{q} u + p \hat{\imath} - \lambda \vec{\delta} (\rho u) \right] = 0 \tag{8}$$

$$\frac{\partial (\rho v)}{\partial t} + \nabla \cdot \left[\rho \vec{q} v + p \hat{\jmath} - \lambda \vec{\delta} (\rho v) \right] = 0 \tag{9}$$

$$\frac{\partial (\rho E)}{\partial t} + \nabla \cdot \left[\rho \vec{q} H - \lambda \vec{\delta} (\rho E) \right] = 0 \tag{10}$$

The notation $\vec{\delta} f$ denotes a change in f in some direction, proportional either to ℓ for first-order dissipation or ℓ^3 for second-order dissipation, ℓ being the cell size. The weight λ is a small coefficient which can take different forms in different upwinding methods, and can also be a matrix to give the characteristic-based or matrix-dissipation methods. These distinctions are not important here.

The additional dissipation terms produce streamwise changes in the entropy, which would otherwise be constant barring truncation errors. The associated entropy source terms can be determined by deriving an expression for the material derivative of the entropy, whose form follows from its definition (6).

$$\begin{aligned} dS &= \frac{\gamma}{\gamma - 1} \frac{dh}{h} - \frac{dp}{p} \\ p\, dS &= \rho\, dH - \rho q\, dq - dp \\ p \frac{DS}{Dt} &= \rho \frac{DH}{Dt} - \rho q \frac{Dq}{Dt} - \frac{Dp}{Dt} \end{aligned} \tag{11}$$

The righthand side terms of equation (11) are determined from the modified momentum and energy equations (8)-(10) by first expanding these as

$$\begin{aligned} \frac{\partial (\rho u)}{\partial t} &+ u \nabla \cdot \left[\rho \vec{q} - \lambda \vec{\delta} \rho \right] + \rho \vec{q} \cdot \nabla u + \frac{\partial p}{\partial x} \\ &= \nabla \cdot \left[\lambda \vec{\delta} (\rho u) \right] - u \nabla \cdot \left[\lambda \vec{\delta} \rho \right] \\ \frac{\partial (\rho v)}{\partial t} &+ v \nabla \cdot \left[\rho \vec{q} - \lambda \vec{\delta} \rho \right] + \rho \vec{q} \cdot \nabla v + \frac{\partial p}{\partial y} \\ &= \nabla \cdot \left[\lambda \vec{\delta} (\rho v) \right] - v \nabla \cdot \left[\lambda \vec{\delta} \rho \right] \\ \frac{\partial (\rho H)}{\partial t} &+ H \nabla \cdot \left[\rho \vec{q} - \lambda \vec{\delta} \rho \right] + \rho \vec{q} \cdot \nabla H - \frac{\partial p}{\partial t} \\ &= \nabla \cdot \left[\lambda \vec{\delta} (\rho E) \right] - H \nabla \cdot \left[\lambda \vec{\delta} \rho \right] \end{aligned}$$

from which follow their corresponding modified convective forms using the modified mass equation.

$$\rho \frac{Du}{Dt} + \frac{\partial p}{\partial x} = \nabla \cdot \left[\lambda \vec{\delta} (\rho u) \right] - u \nabla \cdot \left[\lambda \vec{\delta} \rho \right]$$

$$= \nabla\cdot\left[\lambda\,\rho\,\vec{\delta}u\right] \;+\; \nabla u\cdot\lambda\,\vec{\delta}\rho \qquad (12)$$

$$\rho\frac{Dv}{Dt} + \frac{\partial p}{\partial y} \;=\; \nabla\cdot\left[\lambda\,\vec{\delta}(\rho v)\right] \;-\; v\,\nabla\cdot\left[\lambda\,\vec{\delta}\rho\right]$$

$$= \nabla\cdot\left[\lambda\,\rho\,\vec{\delta}v\right] \;+\; \nabla v\cdot\lambda\,\vec{\delta}\rho \qquad (13)$$

$$\rho\frac{DH}{Dt} - \frac{\partial p}{\partial t} \;=\; \nabla\cdot\left[\lambda\,\vec{\delta}(\rho E)\right] - H\,\nabla\cdot\left[\lambda\,\vec{\delta}\rho\right]$$

$$= \nabla\cdot\left[\lambda\,\rho\,\vec{\delta}H\right] + \nabla H\cdot\lambda\,\vec{\delta}\rho - \nabla\cdot\left[\lambda\,\vec{\delta}p\right] \qquad (14)$$

Combining $(\text{eq.}14) - u(\text{eq.}12) - v(\text{eq.}13)$ produces the desired expression for the convective rate of change of entropy.

$$\rho\frac{DH}{Dt} \;-\; \rho q\frac{Dq}{Dt} \;-\; \frac{Dp}{Dt}$$

$$= \nabla\cdot\left[\lambda\left(\rho\,\vec{\delta}h - \vec{\delta}p\right)\right] \;+\; \nabla h\cdot\lambda\vec{\delta}\rho \;+\; \nabla u\cdot\lambda\rho\,\vec{\delta}u \;+\; \nabla v\cdot\lambda\rho\,\vec{\delta}v \qquad (15)$$

$$p\frac{DS}{Dt} \;=\; \nabla\cdot\left[\lambda\,p\,\vec{\delta}S\right] \;+\; \nabla H\cdot\lambda\vec{\delta}\rho \;+\; \rho^2\left[\nabla u\cdot\lambda\,\vec{\delta}(u/\rho) \;+\; \nabla v\cdot\lambda\,\vec{\delta}(v/\rho)\right] \qquad (16)$$

The first term on the righthand side of equation (16) is simply a diffusion term. The second term is responsible for entropy production in a shock moving through stationary fluid, while the third term is responsible for entropy production in a stationary shock (where H is constant and the second term disappears). For first-order gradient-based dissipation, ∇u and $\vec{\delta}u$ are parallel vectors, so the third term is clearly positive-definite. For the moving shock, the rise in H (or h) is caused by volumetric compression work associated with the change in ρ, so that ∇H and $\vec{\delta}\rho$ are essentially parallel, making the second term is positive definite as well. The net result is that entropy in a numerical solution using gradient-based dissipation increases monotonically downstream, aside from the possibility of lateral diffusion from an adjacent lower-entropy region.

It is useful at this point to examine the effect of using the total enthalpy rather than the total energy to form the dissipation term in the modified energy equation (10).

$$\frac{\partial(\rho E)}{\partial t} \;+\; \nabla\cdot\left[\rho\vec{q}H \;-\; \lambda\,\vec{\delta}(\rho H)\right] \;=\; 0 \qquad (17)$$

This has the advantage of giving perfectly constant H in a steady solution. The entropy transport equation now becomes the following.

$$p\frac{DS}{Dt} \;=\; \nabla\cdot\left[\lambda\,\rho\,\vec{\delta}h\right] \;+\; \nabla H\cdot\lambda\vec{\delta}\rho \;+\; \rho^2\left[\nabla u\cdot\lambda\,\vec{\delta}(u/\rho) \;+\; \nabla v\cdot\lambda\,\vec{\delta}(v/\rho)\right] \qquad (18)$$

The first term on the righthand side is no longer strictly diffusive in the presence of varying pressure gradients, producing non-monotonic entropy evolution along streamlines. This lack of a proper diffusion term also makes the entropy perturbation mode poorly damped, which is consistent with the observation that this form of dissipation is somewhat less stable.

3 Entropy-Conserving Formulation

The approach taken here is to effectively solve the entropy conservation equation (5) in lieu of some combination of the standard mass, momentum, and energy equations. Like the standard equations, the entropy equation must also be stabilized with added "dissipation" (which is not dissipative in the thermodynamic sense). A suitable form is

$$\frac{\partial(\rho S)}{\partial t} \;+\; \nabla\cdot\left[\rho\vec{q}S \;-\; \lambda\,\vec{\delta}(\rho S)\right] \;=\; 0 \qquad (19)$$

which, if employed together with the upwinded mass equation (7), will produce perfectly constant entropy in steady state despite the upwinding.

It is convenient at this point to define shorthand for the residuals appearing in all the conservation equations.

$$\begin{aligned}
R_\rho &\equiv \nabla\cdot\left[\rho\vec{q} \;-\; \lambda\,\vec{\delta}\rho\right] \\
R_u &\equiv \nabla\cdot\left[\rho\vec{q}u \;+\; p\hat{\imath} \;-\; \lambda\,\vec{\delta}(\rho u)\right] \\
R_v &\equiv \nabla\cdot\left[\rho\vec{q}v \;+\; p\hat{\jmath} \;-\; \lambda\,\vec{\delta}(\rho v)\right] \\
R_H &\equiv \nabla\cdot\left[\rho\vec{q}H \;-\; \lambda\,\vec{\delta}(\rho H)\right] \\
R_S &\equiv \nabla\cdot\left[\rho\vec{q}S \;-\; \lambda\,\vec{\delta}(\rho S)\right]
\end{aligned}$$

The formulation will make use of the following convective residuals.

$$\begin{aligned}
R'_u &\equiv R_u \;-\; uR_\rho \\
R'_v &\equiv R_v \;-\; vR_\rho \\
R'_H &\equiv R_H - HR_\rho \\
R'_S &\equiv R_S \;-\; SR_\rho
\end{aligned}$$

These are still discretized in strongly-conservative form as shown, to allow correct shock capturing. It is also convenient at this point to define the convective streamwise and normal momentum residuals.

$$\begin{aligned}
R'_q &= \tfrac{u}{q}\,R'_u \;+\; \tfrac{v}{q}\,R'_v \\
R'_n &= -\tfrac{v}{q}\,R'_u \;+\; \tfrac{u}{q}\,R'_v
\end{aligned}$$

It is readily verified that the following combination is a higher-order quantity.

$$R_\epsilon \;\equiv\; R'_H \;-\; q\,R'_q \;-\; \tfrac{p}{\rho}\,R'_S \;=\; \mathcal{O}\left(|\vec{\delta}|\right) \qquad (20)$$

This simply reflects the fact that S is not an independent variable, so that R'_S must be expressible in terms of the other residuals to within truncation error. With the present gradient-based dissipation, R_ϵ has the following form to leading order.

$$\begin{aligned} R_\epsilon \;=\; & -\nabla \cdot \left[\lambda \vec{\delta p}\right] \;-\; \tfrac{1}{\rho}\nabla p \cdot \left(\lambda \vec{\delta \rho}\right) \\ & -\nabla u \cdot \left(\lambda \rho \, \vec{\delta u}\right) \;-\; \nabla v \cdot \left(\lambda \rho \, \vec{\delta v}\right) \end{aligned} \qquad (21)$$

Since R_ϵ is a higher-order quantity, it is legitimate to set $R_\epsilon = 0$ in relation (20),

$$R'_H \;-\; q\, R'_q \;-\; \tfrac{p}{\rho} R'_S \;=\; 0$$

and then use this relation to replace any one or these three residuals with the remaining two. This is equivalent to adding an appropriate multiple of the dissipation or truncation-error terms, so this modification will preserve consistency. The key idea behind the present scheme is to use the best combination of residuals at every point in the flowfield to maximize accuracy of the discrete solution.

Most of the inaccuracies of conventional Euler solvers are due to their spurious entropy layers which typically form adjacent to surfaces. In the presence of pressure gradients, these layers have displacement effects on the outer potential flow, with the attendant loss of lift, nonzero pressure drag, etc. As shown in the previous section, this spurious entropy production in standard Euler schemes is inevitable, and is arguably their worst feature. Because $R'_S = 0$ implies constant entropy, and $R'_H = 0$ is already being solved, all such spurious entropy production can be eliminated by making the substitution

$$q R'_q \quad \rightarrow \quad R'_H - \tfrac{p}{\rho} R'_S \qquad (22)$$

which discards momentum conservation in favor of entropy conservation. One can consider the switch in equations to be equivalent to adding streamwise momentum sources such that all entropy variations are suppressed. Relation (20) indicates that the change has no effect to within the dissipation or truncation error (i.e. the sources are of higher order) so consistency is unaffected. It is asserted that conserving entropy is preferable in all situations except at shocks, where momentum must be conserved to obtain the correct Rankine-Hugoniot shock jumps.

The substitution (22) is not usable directly, since at a stagnation point where $q = 0$ the entropy is stationary with respect to q (it depends on q^2). Hence, the entropy is not influenced by momentum sources at a stagnation point, so that constant entropy cannot be enforced simply by modifying R'_q in this manner. A singular equation system is produced if this is attempted. The following formulation combines all the equations in a manner which precludes such singularities.

The steady-state equation system for the momentum-conserving case is expressed in vector form as follows.

$$\vec{\mathbf{R}}_{\rm m} \;\equiv\; \left\{ \begin{array}{c} c\, R_\rho \\ R'_u \\ R'_v \\ R'_H \end{array} \right\} \;=\; \mathbf{0} \qquad (23)$$

This will permit correct shock capturing provided the convective residuals are discretized in strongly-conservative form as discussed earlier. The equation switching to the alternative entropy-conserving form is conveniently performed with the unit vector

$$\hat{\mathbf{r}} \;=\; \left\{ \begin{array}{cccc} \frac{g}{G} & \frac{1-g}{G}\frac{u}{q} & \frac{1-g}{G}\frac{v}{q} & 0 \end{array} \right\}^T$$

$$G \;=\; \sqrt{1 - 2g + 2g^2} \qquad (24)$$

where g is a heuristic switch which is 1 near stagnation points (within a distance comparable to the cell size ℓ), and 0 everywhere else.

$$g \;=\; \exp\left[-\left(M/0.05\right)^2\right] \qquad (25)$$

An isentropic (entropy-conserving) residual vector is now defined as

$$\vec{\mathbf{R}}_{\rm is} \;\equiv\; \vec{\mathbf{R}}_{\rm m} \;-\; \hat{\mathbf{r}} \left[\hat{\mathbf{r}} \cdot \vec{\mathbf{R}}_{\rm m} + A\, \tfrac{c}{\gamma} R'_S \right] \qquad (26)$$

$$A \;=\; \tfrac{1-g}{G}\tfrac{c}{q} \;+\; \tfrac{g}{G} \qquad (27)$$

where the weighting factor A merely serves to make the system better-conditioned numerically as $q \rightarrow 0$ and $g \rightarrow 1$ near a stagnation point. Note that

$$\hat{\mathbf{r}} \cdot \vec{\mathbf{R}}_{\rm is} \;=\; -A\, \tfrac{c}{\gamma} R'_S \qquad (28)$$

and A is never zero, so that enforcing $\vec{\mathbf{R}}_{\rm is} = \mathbf{0}$ will force $R'_S = 0$, and produce perfectly isentropic flow.

4 Hybrid Method for Shocks

The momentum-conserving and entropy-conserving residual vectors are now combined into a net residual vector

$$\vec{\mathbf{R}} \;\equiv\; f\, \vec{\mathbf{R}}_{\rm m} \;+\; (1-f)\, \vec{\mathbf{R}}_{\rm is} \;=\; \mathbf{0}$$

where f is a locally-defined "momentum-conservation trigger". If $f = 1$, then the standard momentum-conserving scheme is recovered. If $f = 0$, then entropy is conserved in lieu of streamwise momentum (or in lieu of mass conservation at stagnation points). A more explicit expression for the net residual vector $\vec{\mathbf{R}}$ to be solved is as follows.

$$\begin{aligned}\vec{\mathbf{R}} &= \vec{\mathbf{R}}_{\rm m} \\ &- (1-f)\,\hat{\mathbf{r}}\left[\tfrac{g}{G}\,c\,R_\rho + \tfrac{1-g}{G}R'_q + A\,\tfrac{c}{\gamma}\,R'_S\right] \qquad (29)\end{aligned}$$

It is necessary to examine the consistency and well-posedness of $\vec{\mathbf{R}}$ for intermediate values of f as well as g. This is done by using the following orthogonal basis.

$$\bar{\bar{\mathbf{T}}} \equiv \begin{bmatrix} (1-g) & -g\frac{u}{q} & -g\frac{v}{q} & 0 \\ g & (1-g)\frac{u}{q} & (1-g)\frac{v}{q} & 0 \\ 0 & -\frac{v}{q} & \frac{u}{q} & 0 \\ 0 & 0 & 0 & 1 \end{bmatrix}$$

It is useful to note that $\bar{\bar{\mathbf{T}}}\,\hat{\mathbf{r}} = \{0 \;\; G \;\; 0 \;\; 0\}^T$. Two cases are now considered.

1. Near a shock: $g=0$, f arbitrary.

$$\begin{bmatrix} 1 & 0 & 0 & 0 \\ 0 & q & 0 & 1-f \\ 0 & 0 & 1 & 0 \\ 0 & 0 & 0 & 1 \end{bmatrix} \bar{\bar{\mathbf{T}}}\vec{\mathbf{R}} = \begin{Bmatrix} c\,R_\rho \\ qR'_q + (1-f)R_\epsilon \\ R'_n \\ R'_H \end{Bmatrix}$$

$$\begin{bmatrix} 1 & 0 & 0 & 0 \\ 0 & q & 0 & -f \\ 0 & 0 & 1 & 0 \\ 0 & 0 & 0 & 1 \end{bmatrix} \bar{\bar{\mathbf{T}}}\vec{\mathbf{R}} = \begin{Bmatrix} c\,R_\rho \\ -\frac{p}{\rho}\,R'_S - fR_\epsilon \\ R'_n \\ R'_H \end{Bmatrix}$$

The first form confirms that the method conserves momentum for $f = 1$, while the second confirms that it conserves entropy for $f = 0$. Both forms also show that the method remains consistent for any intermediate value of f, since it multiplies R_ϵ which is a higher-order quantity.

2. Near stagnation: $f=0$, g arbitrary.

$$\begin{bmatrix} q & \frac{g\,c}{GA} & 0 & g \\ 0 & 1 & 0 & 0 \\ 0 & 0 & 1 & 0 \\ 0 & 0 & 0 & 1 \end{bmatrix} \bar{\bar{\mathbf{T}}}\,\vec{\mathbf{R}}_{\rm is} = \begin{Bmatrix} (1-g)qcR_\rho + gR_\epsilon \\ -GA\,\frac{c}{\gamma}\,R'_S \\ R'_n \\ R'_H \end{Bmatrix}$$

Here, the effect of varying $g = 0 \to 1$ is to gradually replace the continuity residual R_ρ with R_ϵ. Again, the system remains consistent for any value of g, except possibly in the limiting case $g=1$, where R_ϵ alone remains. As can be seen from its expansion (21), the leading term of R_ϵ is

$$R_\epsilon = -\nabla\cdot\left[\lambda\,\vec{\delta p}\right] + \ldots$$

which mimics $\nabla^2 p$ for first-order dissipation, and $\nabla^4 p$ for third-order dissipation. In either case, R_ϵ is in effect a regularity constraint on the pressure, and hence plays the same role as the continuity equation which it replaces. The discrete system therefore remains well-posed even for the limiting case $g = 1$, as confirmed by the computed results. This substitution does of course incur a mass-conservation errors near the stagnation point, but these occur over an area which is $\mathcal{O}(\ell^2)$ (essentially one cell) as can be seen from the g definition (24).

A suitable expression for the momentum conservation trigger (a shock-finder, ideally) is based on the undivided convective rate of change of density in the cell.

$$\mathcal{D}_f = \frac{\ell}{\rho c}\,\vec{q}\cdot\nabla\rho \qquad (30)$$

$$f = \begin{cases} 1 - \exp\left[-(1000\,\mathcal{D}_f)^2\right] & ; \quad \mathcal{D}_f > 0 \\ 0 & ; \quad \mathcal{D}_f < 0 \end{cases}$$

Note that an expansion has $\mathcal{D}_f < 0$ and remains isentropic. For unsteady flows, frame-invariant definitions such as

$$\begin{aligned} \mathcal{D}_f &= \frac{\ell}{\rho c}\frac{D\rho}{Dt} \\ \text{or} \quad \mathcal{D}_f &= \frac{\ell}{pc}\frac{Dp}{Dt} \end{aligned}$$

would be preferable to (30). This is a minor distinction here.

5 Solution Method

The solution technique employed here is Newton's method applied directly to the steady residuals (29). At each Newton iteration, the linearized system is solved and the state vector $\vec{\mathbf{U}}$ is updated.

$$\begin{aligned} \left[\frac{\partial\vec{\mathbf{R}}}{\partial\vec{\mathbf{U}}}\right]\delta\vec{\mathbf{U}} &= -\vec{\mathbf{R}} \\ \vec{\mathbf{U}} &\leftarrow \vec{\mathbf{U}} + \delta\vec{\mathbf{U}} \end{aligned}$$

The linear system is solved with GMRES [5], using a sparse ILU solver as a preconditioner [6].

The combined net residual $\vec{\mathbf{R}}$, together with the entropy definition (6) fully determines the time rate of change of the standard conservative-scheme state vector

$$\frac{\partial}{\partial t}\{\rho \;\; \rho u \;\; \rho v \;\; \rho E\}^T$$

for any value of f and g, and therefore can in principle be used with any standard explicit time-marching scheme. Unfortunately, all such explicit schemes have been found to become unstable when entropy is conserved (when $f = 0$). This is perhaps not too surprising, since the residual contributions effectively added to conserve entropy must be anti-dissipative to offset the natural dissipation of the momentum-conserving scheme. The fully-implicit direct Newton solver used here remains stable with this added negative dissipation.

6 Results

The present scheme was implemented in an unstructured grid 2-D Euler code, using grids generated by the FELISA 3-D grid generator [7]. The NACA 0012 airfoil was run using the case parameters tabulated in Table 1. Cases 1a,2a use the conventional momentum-conserving Euler method ($f = 1$ everywhere), while cases 1b,2b use the entropy-conserving formulation ($f = 1$ at shock, $f = 0$ elsewhere). Cases 1a and 1b were also used in a grid-dependence study with the number of grid points on the airfoil perimeter varied from 28 to 112.

Table 1: Test Cases

Case	α	M_∞	surface points	major features
1a,1b	9°	0.30	28,42,70,112	L.E. suction peak
2a,2b	3°	0.80	90	upper-side shock

Figure 1 shows the unstructured grid near the airfoil with 90 surface points. This is a moderately-dense grid for 2-D cases, but it is representative of a section of a rather dense 3-D grid.

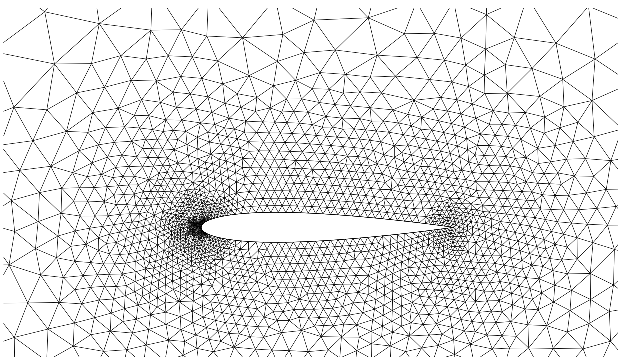

Figure 1: Grid near NACA 0012 airfoil.

6.1 Case 1: Subsonic airfoil

Figure 2 shows the Mach and entropy contours for Case 1a, computed on the 90 surface-point grid. It exhibits the typical entropy layer resulting from numerical dissipation at the strong suction peak, where in this case the local Mach number is just below unity. Figure 3 shows the same case for the entropy-conserving scheme with the same contour levels. The spurious loss is entirely eliminated in the latter case.

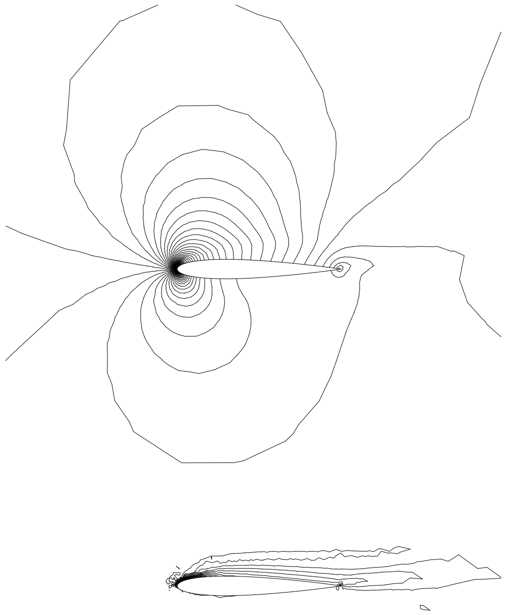

Figure 2: Mach and entropy contours for momentum-conserving Case 1a. NACA 0012 at $\alpha = 9°$, $M_\infty = 0.3$

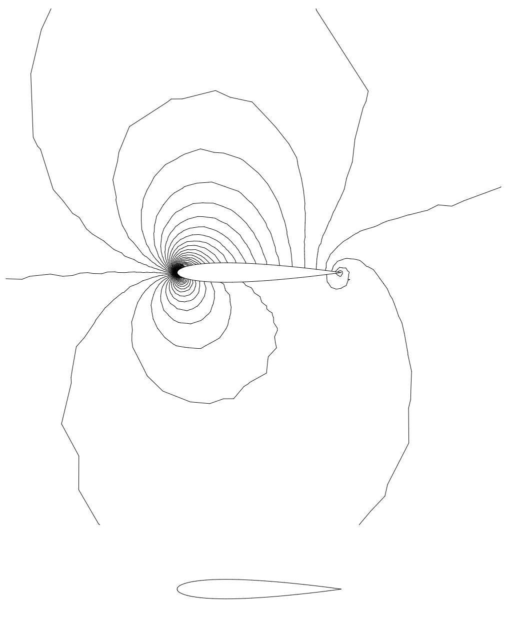

Figure 3: Mach and entropy contours for entropy-conserving Case 1b. NACA 0012 at $\alpha = 9°$, $M_\infty = 0.3$

Figure 4 shows the surface C_p distributions for the four grid densities. In both cases the coarsest grids cannot possibly resolve the sharp leading edge C_p spike. However, the error in the overall lift of the momentum-conserving Case 1a is quite significant, and is apparently due to the displacement effect of the entropy layer acting near the trailing edge. In contrast, the entropy-conserving Case 1b maintains its overall lift much better. Figure 5 shows the C_L and C_D dependence on grid size for the two cases. The entropy layer also causes a very significant spurious pressure drag.

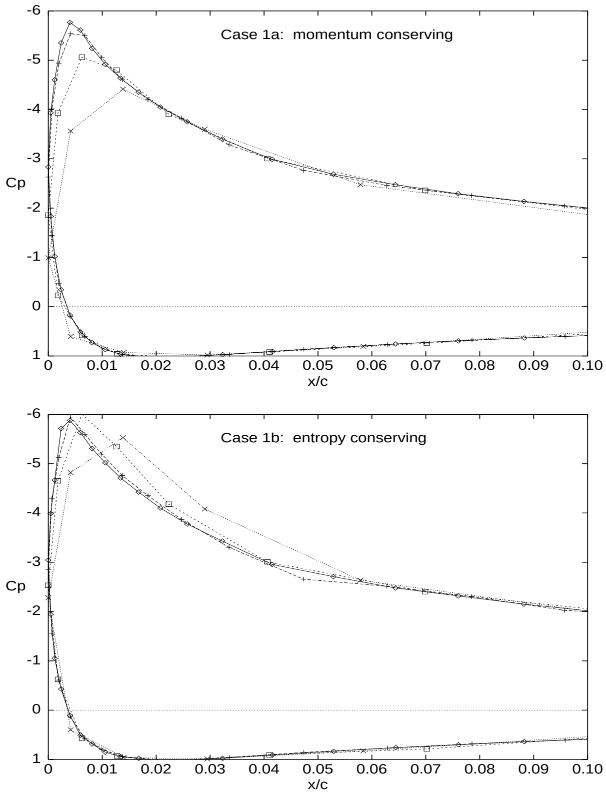

Figure 4: Surface C_p distributions for Case 1a, for four grid densities.

6.2 Transonic airfoil

Figure 6 shows the Mach and entropy contours for Case 2a computed with the conventional Euler method. Roughly the same grid as shown in Figure 1 was used, except that a slightly denser grid was specified over the aft portion of the airfoil to better capture the shock. In addition to the "correct" entropy generated at the shock, the surface entropy layers are also present like in the fully-subsonic Case 1a. Figure 7 shows the result for the entropy-conserving scheme, which allows loss generation only at the shock. Hence, the flow upstream of the shock is strictly isentropic. Figure 8 shows contours of the trigger function f, which is nonzero only at the

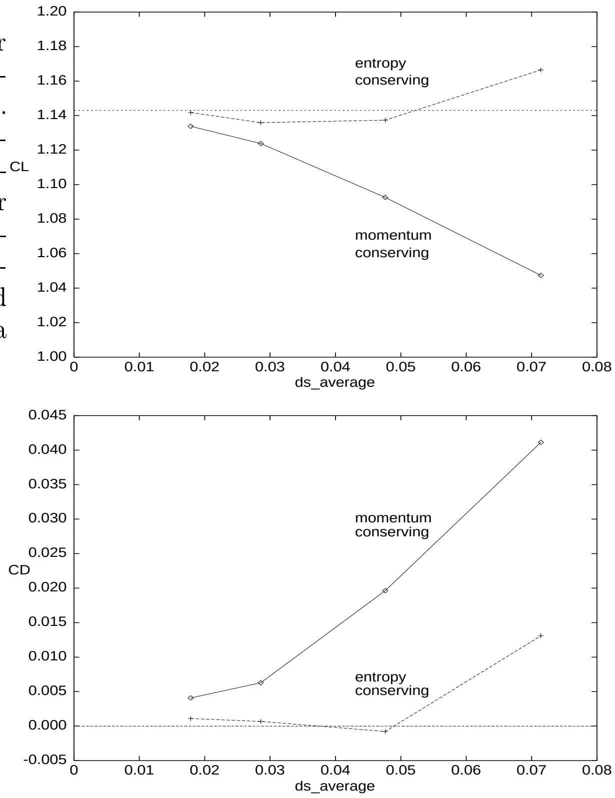

Figure 5: Case 1 C_L and C_D versus average surface cell length (chord = 1).

shock, limiting entropy generation to only that region. Note that once the entropy is generated at the shock itself, it convects and diffuses downstream as usual into the "isentropic" region downstream of the shock. This confirms that the present entropy-conserving scheme merely suppresses entropy *production*. Entropy transport is unaffected as intended.

7 Extensions to Viscous Flows

Current Navier-Stokes methods suffer from much the same spurious entropy production as Euler methods. For viscous flow, this false entropy can be potentially even more destructive, since a false entropy layer in effect adds to the momentum thickness of the real boundary layer and will change its response to pressure gradients. This can in turn cause substantial errors in drag and separation predictions.

The derivation of the present method does not rely on the flow being inviscid. The residual identity (20) is still valid, so that the net modified equation residual vector (29) remains consistent and the overall treatment remains essentially the same. The key difference is that the laminar and Reynolds-averaged shear stress tensor, heat flux, and dissipation are no longer neglected.

$$\bar{\bar{\tau}} \;=\; \mu\left[\nabla\vec{q} + (\nabla\vec{q})^T \;-\; \tfrac{2}{3}\,(\nabla\cdot\vec{q})\,\bar{\bar{\mathrm{I}}}\right] \;-\; \rho\,\overline{\vec{q}\,'\vec{q}\,'^T}$$

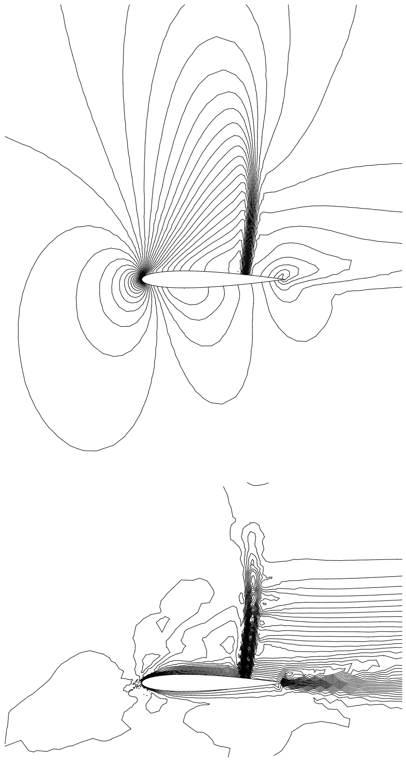

Figure 6: Mach and entropy contours for momentum-conserving Case 2a. NACA 0012 at $\alpha = 3°$, $M_\infty = 0.8$

$$
\begin{aligned}
\vec{Q} &= (\mu/Pr)\,\nabla h \;-\; \rho\,\overline{\vec{q}\,' h'} \\
\varepsilon &= \nabla\cdot(\bar{\bar{\tau}}\cdot\vec{q}) \;-\; \vec{q}\cdot(\nabla\cdot\bar{\bar{\tau}}) \;=\; (\bar{\bar{\tau}}\cdot\nabla)\cdot\vec{q}
\end{aligned}
$$

The momentum, energy, and entropy residuals are now defined as

$$
\begin{aligned}
R_u &= \nabla\cdot\left[\rho\vec{q}u + p\hat{\imath} \;-\; \lambda\,\vec{\delta}(\rho u) \;-\; \bar{\bar{\tau}}\cdot\hat{\imath}\right] \\
R_v &= \nabla\cdot\left[\rho\vec{q}v + p\hat{\jmath} \;-\; \lambda\,\vec{\delta}(\rho v) \;-\; \bar{\bar{\tau}}\cdot\hat{\jmath}\right] \\
R_H &= \nabla\cdot\left[\rho\vec{q}H \;-\; \lambda\,\vec{\delta}(\rho H) \;-\; \bar{\bar{\tau}}\cdot\vec{q} \;-\; \vec{Q}\right] \\
R_S &= \nabla\cdot\left[\rho\vec{q}S \;-\; \lambda\,\vec{\delta}(\rho S)\right] \;-\; \frac{\rho}{p}\left[\varepsilon \;+\; \nabla\cdot\vec{Q}\right]
\end{aligned}
$$

and R_S now has a nonzero source term as expected. Note that this source term is strictly physical and does not directly depend on the upwinding terms, and the accuracy benefits of using R_S are also expected for viscous flows.

8 Extensions to 3-D Flows

The derivation of the present method extends directly to three dimensions, since only an additional z-momentum residual R_w must be introduced. One anticipated change is the likely need to extend the momentum-conservation trigger f to recognize intrinsically dissipative three-dimensional flow features beside shocks. One example is a vortex sheet with streamwise vorticity, typically shed from a wing trailing edge. Momentum must be conserved in the sheet immediately behind the trailing edge so that the appropriate amount of entropy is generated numerically.

9 Conclusions

A method for eliminating spurious losses in Euler equation computations has been presented. The approach can be readily retrofitted to any implicit Euler solver with little additional computational effort, and gives large improvements in accuracy on modest grids. Extensions to viscous and 3-D flows appear feasible.

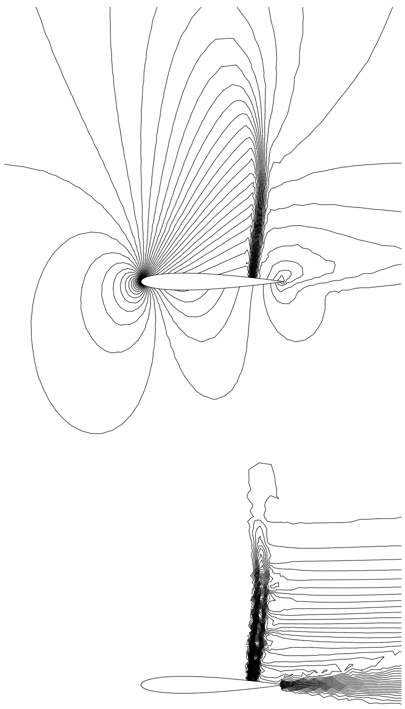

Figure 7: Mach and entropy contours for entropy-conserving Case 2b. NACA 0012 at $\alpha = 3°$, $M_\infty = 0.8$

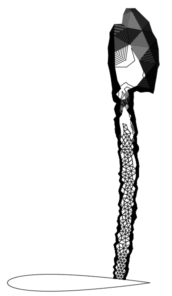

Figure 8: Contours of the trigger function f for Case 2b. Entropy generation occurs only where $f > 0$ at the shock.

References

[1] M. Drela. Newton solution of coupled viscous/inviscid multielement airfoil flows. AIAA 21st Fluid Dyn., Plasma Dyn. and Lasers Conf., Paper AIAA-90-1470, June 1990.

[2] K.D. Lee and S.S Chu. An improvement of convection fidelity in euler calculations. AIAA-89-0473, 1989.

[3] J.D. Denton and L. Xu. A new approach to the calculation of transonic flow through two dimensional turbomachine blade rows. *AMSE 85-GT-5*, Mar 1985.

[4] M. Hafez and W.H. Guo. Simulation of steady compressible flows based on Cauchy/Riemann equations and Crocco's relation. *Intl. J. for Num. Meth. Fluids*, 27:127–138, 1998.

[5] Y. Saad and M.H. Schultz. GMRES: A generalized minimal residual algorithm for solving nonsymmetric linear systems. DCS Report RR-254, Yale University, August 1983.

[6] Y. Saad. SPARSKIT: A basic tool kit for sparse matrix computations, user guide and documentation. (unpublished), 1990.

[7] J. Peraire, J. Peiro, and K. Morgan. Multigrid solution of the 3d compressible euler equations on unstructured tetrahedral grids. *Int. J. for Num. Meth. in Eng.*, 36:1029–1044, 1993.